ASSESSING INTRAURBAN AIR POLLUTION INEQUALITY USING HIGH-RESOLUTION NITROGEN DIOXIDE DATASETS

Mary Angelique G. Demetillo[1], Colin Harkin[2], Brian C. McDonald[2], Kang Sun[3], Phillip S. Chodrow[4], and Sally E. Pusede[1]

[1]Department of Environmental Sciences, University of Virginia, [2]Chemical Sciences Division, NOAA Earth System Research Laboratory, [3]Research and Education in Energy, Environment and Water Institute, University at Buffalo, [4]Department of Mathematics, University of California Los Angeles

Abstract

Redress of air pollution inequality has been limited by the lack of city-wide observations able to resolve steep spatial gradients of trace gas pollutants such as nitrogen dioxide (NO_2). In this paper, I examine the extent of air pollution inequality in 52 major U.S. cities (~130 million residents) using observations from the recently-launched TROPospheric Ozone Monitoring Instrument (TROPOMI) satellite sensor. For each city included in this study, I oversample the first two full years (May 2018 - February 2020) of TROPOMI NO_2 vertical column densities to 0.01° x 0.01° and produce census-tract NO_2 averages and population-weighted NO_2 averages for several sociodemographic groups. I find NO_2 is 36 ± 2% higher for low-income and nonwhite residents (LIN) than for high-income and white residents (HIW) in the largest cities (New York City, NY; Newark, NJ; Los Angeles, CA; Chicago, IL; and Miami, FL) alone.

Introduction and Background

Over 100 million people in the U.S. live in cities where air pollution exceeds standards designated to protect human health.[1] While U.S. air quality has improved over the last few decades, there is evidence that pollutant concentrations are highly variable *within* cities, and disproportionately impact low-income, non-white, and Hispanic communities.[2, 3] Our ability to explain intra-urban variability has been limited by the lack of city-wide, temporally-resolved observations that capture gradients between neighborhoods. For reactive gases with short atmospheric lifetimes, such as nitrogen dioxide (NO_2), intra-urban spatiotemporal variability cannot be directly observed with traditional monitoring approaches, impeding efforts to eliminate disparities through policy.

In Demetillo et al. (2020), I conducted a detailed evaluation of the use of TROPOMI NO_2 observations to describe NO_2 inequality, demonstrating that TROPOMI was indeed well-positioned to inform multiple aspects of intra-urban NO_2 inequality research, at least in the case study city of Houston, Texas. To do this, I used fine spatial resolution (250 m x 500 m) airborne NO_2 remote sensing from the GEOstationary Coastal and Air Pollution Events (GEO-CAPE) Airborne Simulator (GCAS) as a standard (Nowlan et al., 2018; Nowlan et al., 2016), to show that TROPOMI, oversampled to 0.01° x 0.01° using the algorithm employed here, was able to resolve equivalent relative inequalities as the higher resolution GCAS observations. I explored the effects of observational uncertainties, satellite retrieval biases, and time averaging influences on NO_2 inequality estimates, showing that their influence led to underestimations in absolute census-tract-level differences, but TROPOMI was able to resolve significant variations in the intra-urban spatial distribution. Finally, I showed that spatial patterns in NO_2 columns reflected those at the surface, an essential aspect of their application to air quality environmental justice decision-making, and

determined that, at least in Houston, column-based inequalities represented those that would be captured at the surface.

Here, I expand the application of TROPOMI to describe and investigate the sources of NO_2 inequality in 52 major U.S. cities. First, I report neighborhood-level (census-tract) disparities with race, ethnicity, and income observed over an almost two-year period, June 2018–February 2020. I discuss variability of NO_2 inequalities between demographic groups and in NO_2 lifetime.

Data and Methods

TROPOMI

The TROPOspheric Monitoring Instrument (TROPOMI) observes various atmospheric trace gases that absorb in the ultraviolet and visible (270–500 nm), near-infrared (675–775 nm), and shortwave infrared (2305–2385 nm) spectral regions (J. H. G. van Geffen et al., 2018; Veefkind et al., 2012). Onboard the sun-synchronous Copernicus Sentinel-5 Precursor (S5P) satellite, TROPOMI samples at ~1:30 pm local time (LT) almost daily. NO_2 is retrieved by fitting the 405–465 nm band using an updated OMI DOMINO algorithm and based on work from the QA4ECV project (Boersma et al., 2011; Boersma et al., 2018; Lorente et al., 2017; J. H. G. M. van Geffen et al., 2015; Zara et al., 2018). Before 6 August 2019, NO_2 was retrieved at a nadir spatial resolution of 3.5 km x 7 km, NO_2 VCDs have since become available at 3.5 km x 5.5 km (at nadir). Precision of individual tropospheric NO_2 columns over polluted scenes is on the order of 30–60% (Boersma et al., 2018) and dominated by uncertainties in the air mass factor (AMF), with key inputs to the AMF including clouds, the NO_2 profile shape (generated using 1° x 1° TM5-MP model output) (Williams et al., 2017), and the surface albedo from a 0.5° x 0.5° monthly OMI climatology (Kleipool et al., 2008).

I use TROPOMI Level 2 NO_2 tropospheric vertical column densities (VCDs) (J. H. G. van Geffen et al., 2018; Veefkind et al., 2012) averaged to 0.01° x 0.01° (~1 km x 1 km) with a physics-based oversampling algorithm (Sun et al., 2018) for June 2018–February 2020. I include cloud-free scenes with qa > 0.75. I calculate mean NO_2 VCDs within census tract boundaries for 52 U.S. cities, defined as Census-designated 'urbanized areas' (UAs) with two exceptions: I divide the New York City-Newark UA along state lines to create distinct estimates for New York City and Newark and separately analyze inequality within the East Bay boundary from the San Francisco-Oakland UA. Generally speaking, UAs represent the urban core of metropolitan areas; as a result, our results reflect intra-urban rather than urban-suburban differences (Demetillo et al., 2020). To investigate the drivers of NO_2 inequality, I separately analyze NO_2 disparities during the summer (June–August, 2018 and 2019) and winter months (December–February, 2018–2019 and 2019–2020) on weekdays (Tuesday–Friday) and weekends (Saturday–Sunday). Monday and Saturday are considered transition days, and I remove Mondays from our analysis for this reason but keep Saturdays to improve weekend statistics.

NO_X Emissions Inventories

The Fuel-based Inventory from Vehicle Emissions (FIVE) is a U.S. wide (4 km x 4 km) mobile source (on-road + off-road engines) NO_x emission inventory that is temporally resolved (monthly and weekday-weekend) (McDonald et al., 2018). Emission rates are based on publicly available fuel sales reports, road-level traffic counts, and time-resolved weigh-in-motion traffic counts (McDonald et al., 2012). Fuel-use uncertainties are determined from differences between fuel sale reports and truck travel and traffic count site-selection and sample size (±10% for major roads and freeways in large urban areas). Emissions uncertainties are derived from regression analysis of near-road infrared remote sensing and tunnel studies (McDonald et al., 2012).

NO_x stationary source emissions are from the 2017 National Emissions Inventory (NEI) Version 1. The NEI includes emissions from industrial facilities, power plants, airports, and

commercial facilities and combines reports from state, local, and tribal air agencies and the following U.S. Environmental Protection Agency (EPA) programs: Toxic Release Inventory, Acid Rain Program, and Maximum Achievable Control Technology standards development. Emissions uncertainties in power plants are ±25% (Frost et al., 2006); uncertainties in industrial facilities and other stationary sources are larger and assumed to be ±50% (Jiang et al., 2018).

Comparing Population-Weighted Census-Tract NO_2 VCDs

I compute population-weighted NO_2 census-tract-averaged VCDs with race and ethnicity and sort census tracts by household poverty status or household income using the U.S. Census database (Demetillo et al., 2020). Race-ethnicity groups are defined following the U.S. Census: Black and African Americans (JMJE004), Asians (JMJE006), American Indians and Native Alaskans (referred to in the text as Native Americans, JMJE005), and whites (JMJE003), excluding those identifying as Hispanic or Latino, and Hispanics/Latino (JMJE012), including all races reporting as Hispanic. Poverty status is defined as: below the poverty line, >20% of tract households are at or below an income-to-poverty ratio of one (JOCE002 and JOCE003); near the poverty line, all tract households have an income-to-poverty ratio of 1–1.24 (JOCE004); and above the poverty line, all tract households have an income-to-poverty ratio >1.24 (JOCE005, JOCE006, JOCE007, and JOCE008). I combine race-ethnicity and income categories, reporting results for Black and African Americans, Asians, and Native Americans and/or Hispanics/Latinx residents in low-income (lowest income quintile) census tracts (LINs) and for whites (non-Hispanic/Latino) residing in high-income (highest income quintile) tracts (HIWs). Household income quintiles are UA specific. Population-weighted NO_2 columns were calculated as equal to the product of the tract-unit NO_2 column ($NO_{2,j}$) and demographic group population (p_j) (by race-ethnicity or poverty classification) in the i^{th} tract, summed over all census tracts with NO_2 data (n), and divided by the summation of the group population (p_j) (Eq. 1). Errors were defined as standard mean errors, with N representing the number of census tracts with both NO_2 observations and residents of a given demographic group:

$$(1) \qquad P_j = \sum_{i=1}^{n} NO_{2,j}\, p_{i,j} \,/\, \sum_{i=1}^{n} p_{i,j}$$

Results

For the 130 million residents of the U.S. cities in our study, population-weighted NO2 VCDs are 12 ± 2% higher for Black and African Americans, 13 ± 2% higher for Hispanic/Latino, 6 ± 2% greater for Asians, and 10 ± 2% higher for Native Americans compared to whites. I observe higher population-weighted NO2 for people below (14 ± 2%) and near the poverty line (8 ± 2%) than those above the poverty line. When race-ethnicity and income are combined, I report 22 ± 2% greater population-weighted NO_2 for LINs than HIWs (Table 1).

Table 1. Table of Coarse-TROPOMI Weighted-Average (Across all 50 UAs in this Study) Population-Weighted NO_2 Means (x10^{15} molecules cm^{-2}) by Sociodemographic Group Overall (All Days from June 2018–February 2020), During Summer (June–August) Weekdays and Weekends, and During Winter (December–February) Weekdays and Weekends. Uncertainties are 1σ.

	Overall	Summer Weekday	Summer Weekend	Winter Weekday	Winter Weekend
Below	3.6 ± 1.0	3.3 ± 1.0	2.5 ± 1.0	5.1 ± 1.0	4.5 ± 1.0
Near	3.1 ± 1.0	2.9 ± 1.0	2.3 ± 1.0	4.5 ± 1.0	4.1 ± 1.0
Above	2.8 ± 0.8	2.6 ± 0.8	2.1 ± 0.8	4.0 ± 0.8	3.8 ± 0.8
White	2.7 ± 0.7	2.4 ± 0.7	2.0 ± 0.7	3.7 ± 0.7	3.6 ± 0.7
Black or African American	3.3 ± 1.0	3.0 ± 1.0	2.4 ± 1.0	4.8 ± 1.0	4.3 ± 1.0
Asian	3.0 ± 0.9	2.8 ± 0.9	2.2 ± 0.9	4.2 ± 0.9	4.1 ± 0.9
Hispanic	3.2 ± 1.0	3.0 ± 1.0	2.3 ± 1.0	4.6 ± 1.0	4.2 ± 1.0
Native American	3.0 ± 0.9	2.8 ± 0.9	2.2 ± 0.9	4.4 ± 0.9	3.9 ± 0.9
LIN	3.5 ± 1.1	3.3 ± 1.1	2.5 ± 1.1	5.1 ± 1.1	4.4 ± 1.1
HIW	2.6 ± 0.7	2.4 ± 0.7	1.9 ± 0.7	3.5 ± 0.7	3.5 ± 0.7

The highest inequalities were observed in Newark, New Jersey (50 ± 2%) and Los Angeles, California (49 ± 1%) and the lowest inequalities were observed in San Francisco, California (2 ± 3%) and New Orleans, Louisiana (4 ± 3%) (Figure 1). Inequality is higher in the largest U.S. cities, with 36 ± 2% higher NO_2 for LINs compared to HIWs in the five most-populated UAs, New York City, Newark, Los Angeles, Chicago, and Miami, representing ~35% of the population in our domain.

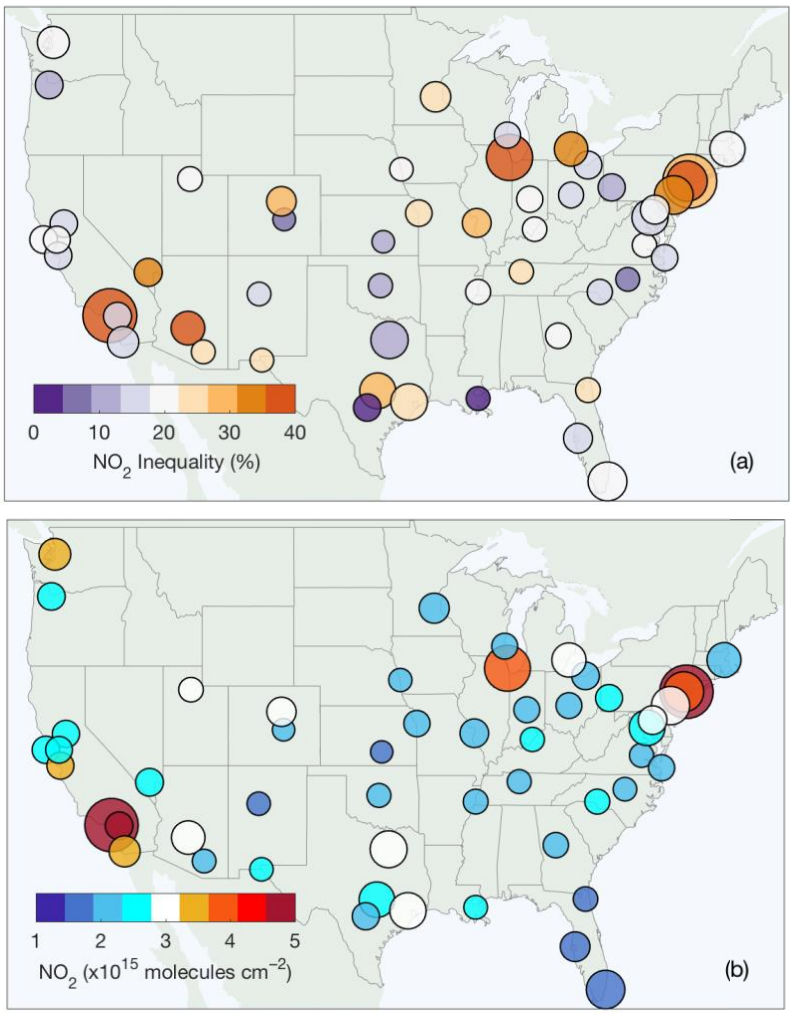

Figure 1. (a) Average city NO_2 inequality and (b) NO_2 for 52 major U.S. cities over all days in the study (June 2018–February 2020). Marker size reflects the total city population with the smallest markers representing cities with fewer than 1.5 million residents and the largest markers for cities with more than 10 million residents.

NO_2 inequality was strongly associated with city-level NO_2 pollution (Figure 1). I quantify this relationship for the combined race-ethnicity and income metric (LIN-HIW), by fitting absolute inequalities versus mean NO_2 VCD for the 52 cities using a weighted bivariate linear regression model (York et al., 2004) in the summer and winter months separately. I find that NO_2 inequality is better correlated with (r^2 = 0.86) and more sensitive to (slope = 0.53 ± 0.02) city-level NO_2 in the summer when the NO_2 atmospheric lifetime is short. In the winter, I observe more variance in the correlation (r^2 = 0.58) and less sensitivity to (slope = 0.33 ± 0.01) the overall NO_2 concentrations. In addition, I observe that absolute inequality is better correlated with city-wide NO_2 than relative inequality. Correlation coefficients between relative disparities and mean NO_2 fall to 0.57 and 0.04 in the summer and winter, respectively, implying that even with sustained NO_x emission controls and decreased urban NO_2 pollution, relative inequalities will persist.

Conclusions and Next Steps

I demonstrate TROPOMI's ability to resolve differences in NO_2 between sociodemographic groups at the neighborhood-level within ~50 major cities in the contiguous U.S. Heavy-duty diesel vehicles (HDDVs) have been shown to drive air pollution inequalities and contribute to health disparities in U.S. cities (Demetillo et al., 2020; Houston et al., 2008; Houston et al.,

2014; Houston et al., 2011; Lena et al., 2002; J. I. Levy et al., 2009; Nguyen & Marshall, 2018). HDDVs are responsible for a major portion of the NO_x emissions in many urban areas (McDonald et al., 2012), despite the fact that they are a small fraction (3–6%) of the U.S. fleet, as diesel engines produce seven times more NO_x per kg fuel burned than gasoline (McDonald et al., 2018). To investigate the contribution of HDDVs to inequality, I will compare absolute NO_2 inequality on weekdays and weekends using both TROPOMI observations and emissions inventory NO_x estimates.

References

Apte, J. S., Messier, K. P., Gani, S., Brauer, M., Kirchstetter, T. W., Lunden, M. M., et al. (2017). High-Resolution Air Pollution Mapping with Google Street View Cars: Exploiting Big Data. *Environmental Science & Technology, 51*(12), 6999-7008. https://doi.org/10.1021/acs.est.7b00891

Boersma, K. F., Eskes, H. J., Dirksen, R. J., van der A, R. J., Veefkind, J. P., Stammes, P., et al. (2011). An improved tropospheric NO₂ column retrieval algorithm for the Ozone Monitoring Instrument. *Atmos. Meas. Tech., 4*(9), 1905-1928. https://www.atmos-meas-tech.net/4/1905/2011/

Boersma, K. F., Eskes, H. J., Richter, A., De Smedt, I., Lorente, A., Beirle, S., et al. (2018). Improving algorithms and uncertainty estimates for satellite NO2 retrievals: results from the quality assurance for the essential climate variables (QA4ECV) project. *Atmos. Meas. Tech., 11*(12), 6651-6678. https://www.atmos-meas-tech.net/11/6651/2018/

Clark, L. P.; Millet, D. B.; Marshall, J. D. National Patterns in Environmental Injustice and Inequality: Outdoor NO2 Air Pollution in the United States. *PLoS One* **2014,** *9* (4).

Chodrow, P. S. (2017). Structure and information in spatial segregation. *Proceedings of the National Academy of Sciences, 114*(44), 11591-11596. https://www.pnas.org/content/pnas/114/44/11591.full.pdf

Council, N. R. (2001). *America Becoming: Racial Trends and Their Consequences: Volume I*. Washington, DC: The National Academies Press.

Demetillo, M. A. G., Navarro, A., Knowles, K. K., Fields, K. P., Geddes, J. A., Nowlan, C. R., et al. (2020). Observing Nitrogen Dioxide Air Pollution Inequality Using High-Spatial-Resolution Remote Sensing Measurements in Houston, Texas. *Environmental Science & Technology*. https://doi.org/10.1021/acs.est.0c01864

Frost, G. J., McKeen, S. A., Trainer, M., Ryerson, T. B., Neuman, J. A., Roberts, J. M., et al. (2006). Effects of changing power plant NOx emissions on ozone in the eastern United States: Proof of concept. *Journal of Geophysical Research: Atmospheres, 111*(D12). https://agupubs.onlinelibrary.wiley.com/doi/abs/10.1029/2005JD006354

Houston, D., Krudysz, M., & Winer, A. (2008). Diesel Truck Traffic in Low-Income and Minority Communities Adjacent to Ports:Environmental Justice Implications of Near-Roadway Land Use Conflicts. *Transportation Research Record, 2067*(1), 38-46. https://journals.sagepub.com/doi/abs/10.3141/2067-05

Houston, D., Li, W., & Wu, J. (2014). Disparities in Exposure to Automobile and Truck Traffic and Vehicle Emissions Near the Los Angeles–Long Beach Port Complex. *American Journal of Public Health, 104*(1), 156-164. https://ajph.aphapublications.org/doi/abs/10.2105/AJPH.2012.301120

Houston, D., Ong, P., Jaimes, G., & Winer, A. (2011). Traffic exposure near the Los Angeles–Long Beach port complex: using GPS-enhanced tracking to assess the implications of unreported travel and locations. *Journal of Transport Geography, 19*(6), 1399-1409. http://www.sciencedirect.com/science/article/pii/S0966692311001347

Institute, H. E. (2010). Traffic-Related Air Pollution: A Critical Review of the Literature on Emissions, Exposure, and Health Effects. (Special Report 17).

Jiang, Z., McDonald, B. C., Worden, H., Worden, J. R., Miyazaki, K., Qu, Z., et al. (2018). Unexpected slowdown of US pollutant emission reduction in the past decade. *Proceedings of the National Academy of Sciences, 115*(20), 5099-5104. https://www.pnas.org/content/pnas/115/20/5099.full.pdf

Kleipool, Q. L., Dobber, M. R., de Haan, J. F., & Levelt, P. F. (2008). Earth surface reflectance climatology from 3 years of OMI data. *Journal of Geophysical Research: Atmospheres, 113*(D18). https://agupubs.onlinelibrary.wiley.com/doi/abs/10.1029/2008JD010290

Lee, B. A., Reardon, S. F., Firebaugh, G., Farrell, C. R., Matthews, S. A., & O'Sullivan, D. (2008). Beyond the Census Tract: Patterns and Determinants of Racial Segregation at Multiple Geographic Scales. *American Sociological Review, 73*(5), 766-791. Lena, T. S., Ochieng, V., Carter, M., Holguín-Veras, J., & Kinney, P. L. (2002). Elemental carbon and PM(2.5)levels in an urban community heavily impacted by truck traffic. *Environmental Health Perspectives, 110*(10), 1009-1015.

Levy, I., Mihele, C., Lu, G., Narayan, J., & Brook, J. R. (2014). Evaluating Multipollutant Exposure and Urban Air Quality: Pollutant Interrelationships, Neighborhood Variability, and Nitrogen Dioxide as a Proxy Pollutant. *Environmental Health Perspectives*, *122*(1), 65-72.

Levy, J. I., Greco, S. L., Melly, S. J., & Mukhi, N. (2009). Evaluating Efficiency-Equality Tradeoffs for Mobile Source Control Strategies in an Urban Area. *Risk Analysis*, *29*(1), 34-47. https://onlinelibrary.wiley.com/doi/abs/10.1111/j.1539-6924.2008.01119.x

Lorente, A., Folkert Boersma, K., Yu, H., Dörner, S., Hilboll, A., Richter, A., et al. (2017). Structural uncertainty in air mass factor calculation for NO2 and HCHO satellite retrievals. *Atmos. Meas. Tech.*, *10*(3), 759-782. https://www.atmos-meas-tech.net/10/759/2017/

Marr, L. C., & Harley, R. A. (2002). Modeling the Effect of Weekday−Weekend Differences in Motor Vehicle Emissions on Photochemical Air Pollution in Central California. *Environmental Science & Technology*, *36*(19), 4099-4106. https://doi.org/10.1021/es020629x

McDonald, B. C., Dallmann, T. R., Martin, E. W., & Harley, R. A. (2012). Long-term trends in nitrogen oxide emissions from motor vehicles at national, state, and air basin scales. *Journal of Geophysical Research: Atmospheres*, *117*(D21). https://agupubs.onlinelibrary.wiley.com/doi/abs/10.1029/2012JD018304

McDonald, B. C., McKeen, S. A., Cui, Y. Y., Ahmadov, R., Kim, S.-W., Frost, G. J., et al. (2018). Modeling Ozone in the Eastern U.S. using a Fuel-Based Mobile Source Emissions Inventory. *Environmental Science & Technology*, *52*(13), 7360-7370. https://doi.org/10.1021/acs.est.8b00778

Nguyen, N. P., & Marshall, J. D. (2018). Impact, efficiency, inequality, and injustice of urban air pollution: variability by emission location. *Environmental Research Letters*, *13*(2), 024002. http://dx.doi.org/10.1088/1748-9326/aa9cb5

Nowlan, C. R., Liu, X., Janz, S. J., Kowalewski, M. G., Chance, K., Follette-Cook, M. B., et al. (2018). Nitrogen dioxide and formaldehyde measurements from the GEOstationary Coastal and Air Pollution Events (GEO-CAPE) Airborne Simulator over Houston, Texas. *Atmos. Meas. Tech.*, *11*(11), 5941-5964. https://amt.copernicus.org/articles/11/5941/2018/

Nowlan, C. R., Liu, X., Leitch, J. W., Chance, K., González Abad, G., Liu, C., et al. (2016). Nitrogen dioxide observations from the Geostationary Trace gas and Aerosol Sensor Optimization (GeoTASO) airborne instrument: Retrieval algorithm and measurements during DISCOVER-AQ Texas 2013. *Atmos. Meas. Tech.*, *9*(6), 2647-2668. https://www.atmos-meas-tech.net/9/2647/2016/

Reardon, S. F., & O'Sullivan, D. (2004). Measures of Spatial Segregation. *Sociological Methodology*, *34*(1), 121-162. https://onlinelibrary.wiley.com/doi/abs/10.1111/j.0081-1750.2004.00150.x

Sun, K., Zhu, L., Cady-Pereira, K., Chan Miller, C., Chance, K., Clarisse, L., et al. (2018). A physics-based approach to oversample multi-satellite, multispecies observations to a common grid. *Atmos. Meas. Tech.*, *11*(12), 6679-6701. https://www.atmos-meas-tech.net/11/6679/2018/

Tessum, C. W.; Apte, J. S.; Goodkind, A. L.; Muller, N. Z.; Mullins, K. A.; Paolella, D. A.; Polasky, S.; Springer, N. P.; Thakrar, S. K.; Marshall, J. D.; Hill, J. D. Inequity in Consumption of Goods and Services adds to Racial–Ethnic Disparities in Air Pollution Exposure. *Proc. Natl. Acad. Sci. U.S.A* **2019,** *116* (13), 6001.

USGCRP *Impacts, Risks and Adaptation in the United States: Fourth National Climate Assessment, Volume II*; U.S. Global Change Research Program: Washington, D.C., USA, 2018; p 1515.

van Geffen, J. H. G., Boersma, K. F., Eskes, H. J., Maasakkers, J. D., & Veefkind, J. P. (2018). TROPOMI ATBD of the total and tropospheric NO2 data products. Retrieved from http://www.tropomi.eu

van Geffen, J. H. G. M., Boersma, K. F., Van Roozendael, M., Hendrick, F., Mahieu, E., De Smedt, I., et al. (2015). Improved spectral fitting of nitrogen dioxide from OMI in the 405–465 nm window. *Atmos. Meas. Tech.*, *8*(4), 1685-1699. https://www.atmos-meas-tech.net/8/1685/2015/

Veefkind, J. P., Aben, I., McMullan, K., Förster, H., de Vries, J., Otter, G., et al. (2012). TROPOMI on the ESA Sentinel-5 Precursor: A GMES mission for global observations of the atmospheric composition for climate, air quality and ozone layer applications. *Remote Sensing of Environment*, *120*, 70-83. http://www.sciencedirect.com/science/article/pii/S0034425712000661

Williams, J. E., Boersma, K. F., Le Sager, P., & Verstraeten, W. W. (2017). The high-resolution version of TM5-MP for optimized satellite retrievals: description and validation. *Geosci. Model Dev.*, *10*(2), 721-750. https://www.geosci-model-dev.net/10/721/2017/

York, D., Evensen, N. M., Martínez, M. L., & Delgado, J. D. B. (2004). Unified Equations for the Slope, Intercept, and Standard Errors of the Best Straight

Line. *Amer. J. Phys.*, *72*(3), 367-375. https://aapt.scitation.org/doi/abs/10.1119/1.1632486

Zara, M., Boersma, K. F., De Smedt, I., Richter, A., Peters, E., van Geffen, J. H. G. M., et al. (2018). Improved slant column density retrieval of nitrogen dioxide and formaldehyde for OMI and GOME-2A from QA4ECV: intercomparison, uncertainty characterisation, and trends. *Atmos. Meas. Tech.*, *11*(7), 4033-4058. https://www.atmos-meas-tech.net/11/4033/2018/